DIAGNOSTYKA, 2024, Vol. 25, No. 1

e-ISSN 2449-5220
DOI: 10.29354/diag/181192

TIME - FREQUENCY METHOD AND ARTIFICIAL NEURAL NETWORK CLASSIFIER FOR INDUCTION MOTOR DRIVE SYSTEM DEFECTS CLASSIFICATION

Meriem BEHIM , Leila MERABET , Salah SAAD *

LSEM, Laboratoire des Systèmes Electromécaniques, Badji Mokhtar University, 23000 Annaba, B.O 12, Algeria.
* Corresponding author: saadsalah2006@yahoo.fr

Abstract

In this paper, by introducing two statistical parameters, energy and L-kurtosis, a new fault diagnostic system combining Wavelet Packet Decomposition and Multilayer Perceptron Neural Network is designed to improve efficiency and precision of induction motor defects diagnosis. This method is applied to vibratory signals of asynchronous motor running at two different rotational speeds (1500 rpm and 2000 rpm) at a sampling frequency of 8 KHz to detect three main types of defects: bearing faults, load imbalance and misalignment. These speeds are considered as the usual medium running speeds of induction motor. According to the results, the high performance and accuracy of this new faults diagnostic system is proved and confirmed, thus it can be used in the detection of other machines defects.

Keywords: Energy, L-kurtosis, Wavelet Packet Decomposition, Multilayer Perceptron Neural Network, Induction motor defects, Vibratory signals

1. INTRODUCTION

Despite the development which affects all fields, induction motors remain essential machines in the industrial world, and researchers are constantly investigating these machines and developing diagnostic methods in order to ensure their availability. Several studies have shown that the Induction motor (IM) mechanical defects represent a great rate of the hole defects that can occur on these motors, where the bearing defects, only, stand for more than 40% of the total rate [1]. However, most of the researches were focused on diagnosing bearing faults on the breakage side of the outer ring, inner ring, cage and balls; let us cite for example the work of [2] whose the exploited method is a combination of kurtogram, wavelet packet transform and iterative 1.5-dimensional spectrum; and in [3] the researcher has exploited wavelet energy entropy and least square support vector machine as method for fault diagnosis; while in [4], the researchers proposed dilated convolution neural network based model to detect both bearing faults and broken rotor bar; and in [5], the authors have combined wavelet packet transform with convolution neural network optimized by simulated annealing algorithm; when in [6] the proposed method was based on an improved convolution neural network called multiple fault convolution neural network classifier (MFCNN). Although in reality, bearing defects are not limited to these types of defects, in others terms these defects are the result of other factors such as: lack of lubrication, improper lubricant, imbalances, misalignment, etc.

According to the literature, many works have widely investigated these types of defects such as reported in [7] where the author studied the improper lubrication defect using the Wavelet Packet Decomposition (WPD) method. Whereas, the authors of [8–10] focused their work on the misalignment defect using wavelet transform and multiscale entropy, multi-input convolution neural network, and Fast Fourier Transform (FFT) with Support Vector Machine (SVM) respectively. The load unbalance defect was treated in [11] based on wavelet packet decomposition and power spectral density. While there isn't a single comprehensive work that addresses all of these defects simultaneously.

Furthermore, in recent years, researches dealing with defects diagnosis in rotating machines, in general, go towards the combination of artificial intelligent (AI) techniques and time-frequency methods as presented by the authors of [12 -13]. It is for this reason that this work aims to study five types of defects (load unbalance, parallel misalignment, improper lubrication, lack of lubrication, combined defects of broken cage + lack of lubrication) not

Received 2023-06-07; Accepted 2024-01-15; Available online 2024-01-28

widely investigated previously using a novel methodology based on the WPD energy, Multilayer Perceptron Neural Network (MLP-NN) and statistical parameter L-kurtosis. WPD represents the best time-frequency method due to its better resolution over other time-frequency approaches and its ability to decompose both high and low frequencies of the considered signal, whereas MLP-NN is the easiest and most popular AI technique for its application; and the statistical parameter L-kurtosis is introduced as simple indicator switch the variation of its values used to indicate the defects as presented in [14–16], but not considered previously as a feature of classification despite its precision and its robustness to outliers.

The main contributions of this work are: The classification of various and combined defects of IM that have not been largely investigated (load unbalance, parallel misalignment, improper lubrication, lack of lubrication, combined defects of (broken cage + lack of lubrication). Adding to this, the integration of a novel feature (L-kurtosis) extracted from WPD to train MLP-NN classifier in order to diagnose several IM defects. Finally, a data gathering system was used to evaluate the suggested methodology at two different motor rotational speeds.

The main challenge of this methodology is its capability to detect other combined defects using shorter signals.

For comparison, Table 1 summarizes the contribution of the proposed methodology of some works cited above.

In this paper the theoretical background of induction motor defects, WPD energy, L-kurtosis and MLP-NN are presented. The proposed methodology, data acquisitions (vibratory signals) system and the results are discussed and analyzed.

2.THEORETICAL BACKGROUND

2.1. Induction motor defects impact on vibration signal

Vibration techniques are usually used for mechanical fault detection, depending on the data given by vibratory signals, using sensors. Hence, there are three types of sensors[17]: acceleration sensors; speed sensors are confined in their capability to accurately measure speed within a specific frequency range due to their limited low-frequency response: and displacement sensors which are electrical eddy current sensors with non-contact measurement.

The various vibration data gathered are used to identify and validate different defects[18].

In the present paper three types of defects are treated: mechanical load unbalance, parallel misalignment and lubrication and cage bearing defect.

Mechanical load unbalance

The mechanical load unbalance defect is defined as a non-uniform distribution of the mass around an axis of rotation by placing additional weights on a balanced metal disk as presented in Fig.1. This mass causes a centrifugal force that causes torque

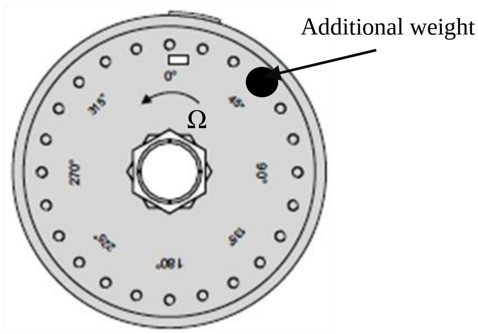

Fig. 1. Load unbalance

Table 1. Comparison of different fault detecting techniques

Reference	Fault types	Exploited methods	Results / Accuracy
[7]	Improper lubrication	WPD	It was concluded that, for medium speeds DWT decomposition procedure is efficient to distinguish between improper lubricated bearing and healthy bearing.
[8]	Misalignment defect	WT, multiscale entropy, SVM	The highest accuracy is 91.1%
[9]	Misalignment defect Crack in rotor System	multi-input CNN	Classification accuracy is 99.42%
[10]	Misalignment defect	FFT, SVM	Classification accuracy is 98.8%
[11]	Load unbalance	WPD energy, power spectral density	The ability of the proposed method to separate between healthy state and load unbalance defect with different severity levels
The present work	Load unbalance Parallel misalignment Improper lubrication Lack of lubrication Combined defects of broken cage + lack of lubrication	WPD energy, L-kurtosis and MLP-NN	High accuracy of 100% is obtained when dealing with different defect types

oscillations at specific frequencies that are frequently correlated with the mechanical speed of the motor. [11]. According to [19], within the vibration analysis, the amplitude of the motor speed decreases with load increase.

Misalignment

When the driven machine shaft and the drive machine shaft are not on the same centerline, this is referred to as misalignment. According to Fig. 2, there are three different forms of misalignment: parallel, angular, and general [20].

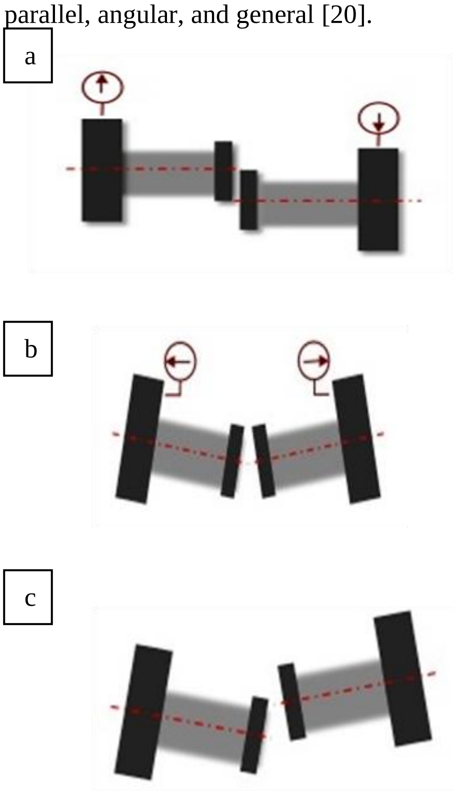

Fig. 2. Misalignment: a) parallel, b) angular, c) general

Bearing defect

The statistical study of IM's defects indicate that bearings failures represent more than forty percent of the IM defects. These defects can occur on several components of the rolling element bearing (inner (IR) and outer races (OR), rolling elements (B) and cages (C)) [18], [21], [22] as shown in Fig.3 due to several factors such as lubrication failure, bearing overheating, corrosion and contamination, excessive load, and incorrect assembly and misalignment.

Bearing issues appears in additional frequencies (f) that express each type of defect as follows:

$$\begin{cases} f_{OR}\,(Hz) = \frac{Z}{2} f_r (1 - \frac{B_D}{C_D} cos\beta) \\ f_{IR}\,(Hz) = \frac{Z}{2} f_r (1 + \frac{B_D}{C_D} cos\beta) \\ f_B\,(Hz) = f_r \frac{C_D}{2B_D}\left[1 - \left(\frac{B_D}{C_D} cos\beta\right)^2\right] \\ f_c(Hz) = \frac{f_r}{2}(1 - \frac{B_D}{C_D} cos\beta) \end{cases} \quad (1)$$

Where: Z: rollers' number, B_D: ball diameter, C_D: pitch circle diameter, β: angle of contact (rad), and f_r: rotating frequency.

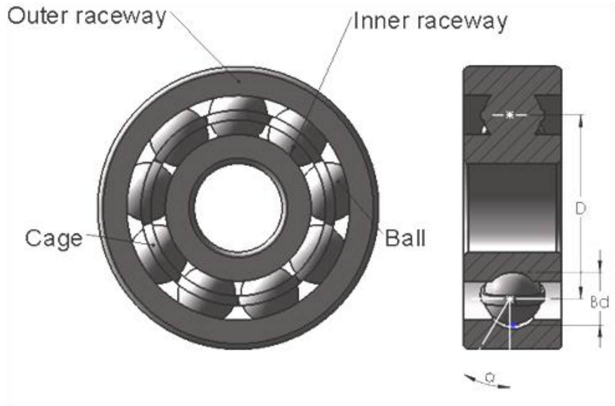

Fig. 3. Bearing components

2.2. Wavelet packet decomposition energy

A signal processing technique with resolution that adapts to the size of the object or the examined information is the wavelet transform (WT) [23]. This method divides the signal into smaller components known as wavelets, which have the property of being well localizable in time or frequency because of their fundamental building blocks, generated by translation b and dilatation a from a function, mother wavelet[24].

$$\Psi_{a,b}(t) = \frac{1}{\sqrt{a}}\Psi\left(\frac{t-b}{a}\right) \quad (2)$$

Contrary to discreet and continuous wavelet transform, the Coifman and Wickerhauser WPD generates at each level an approximation coefficient containing low frequency information and a detail coefficient containing high frequency information of the original signal without data loss or redundancy. The procedure can be carried out multiple times to create the tree structure depicted in Fig. 4. [11], [25].

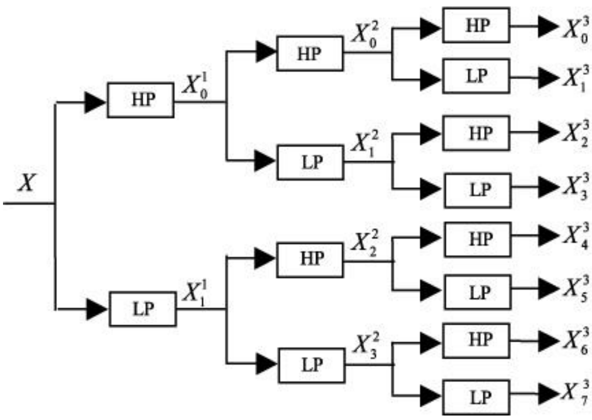

Fig. 4. WPD tree with depth of 3

The WPD coefficients X_k^{j+1} are defined by[26]:

$$\begin{cases} X_{2p}^{j+1}[n] = \sum_m HP[m-2n]X_p^j[m] \\ X_{2p+1}^{j+1}[n] = \sum_m LP[m-2n]X_p^j[m] \end{cases} \quad (3)$$

With: p=0,1,2...,2^{j-1} : Numbered nodes of level j. (4)

The energy eigenvalue of each frequency band at a decomposition level j, is given by [27]:

$$E_j = \sum_{n=1}^{N} \left|X_j(n)\right|^2 \quad (5)$$

where: $X_j(n)$ are the wavelet packet coefficients.

2.3.L-kurtosis

L-kurtosis is the extended form of the traditional kurtosis, it is more accurate in estimating parameters and more reliable against outliers[28].

L-kurtosis represents the fourth order L-moment; it is defined as [29]:

$$L\_Kurtosis = \frac{L_4}{L_2} \quad (6)$$

Where:

$$L_r = \frac{1}{r}\sum_{k=0}^{r-1}(-1)^k \binom{r-1}{k} E(x_{r-k:r}) \quad (7)$$

With: ($x_{1:N}$) independent sample ranked in ascending order from 1 to n with the cumulative distribution function P(x) and quantile function x(P); r: L-moment order, and $E(x_{r-k:r})$: the expectation of the r-k order statistic of a sample of size r:

$$E(x_{j:r}) = \frac{r!}{(j-1)!(r-j)!}\int_0^1 x(P)[P(x)]^{j-1}[1-P(x)]^{r-j}\,dP(x) \quad (8)$$

In case of discreet data ($x_{1:N}$) , ranked in ascending order from 1 to n, L_4 and L_2 will be defined as [30]:

$$\begin{cases} L_4 = 20\beta_3 - 30\beta_2 + 12\beta_1 - \beta_0 \\ L_2 = 2\beta_1 - \beta_0 \end{cases} \quad (9)$$

Where:

$$\begin{cases} \beta_0 = N^{-1}\sum_{i=1}^{N} x_i \\ \beta_1 = N^{-1}\sum_{i=2}^{N} x_i \left[\frac{(i-1)}{(N-1)}\right] \\ \beta_2 = N^{-1}\sum_{i=3}^{N} x_i \left[\frac{(i-1)(i-2)}{(N-1)(N-2)}\right] \\ \beta_2 = N^{-1}\sum_{i=4}^{N} x_i \left[\frac{(i-1)(i-2)(i-3)}{(N-1)(N-2)(N-3)}\right] \end{cases} \quad (10)$$

2.4. Multi-Layer Perceptron neural network

The most often used MLP-NN is made up of an input layer, whose nodes' numbers are proportional to the number of input data, one or more hidden layers, and an output layer. The resultant data from each layer represents entries for the following layer switch a set of appropriate rules and algorithms [31-32], as illustrated in Fig. 5.

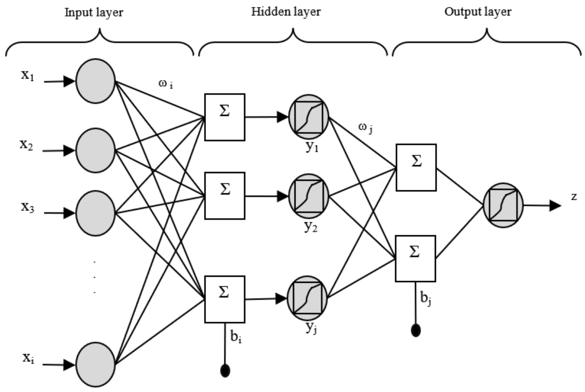

Fig. 5. MLP-NN architecture

Where: x_i
and ω_j the weights, b_i and b_j: the bias, z: the output and

The most popular activation functions used for the MLP-NN classifier are:

Tangent Sigmoïde function (TanSig):

$$TanSig(x) = \frac{2}{1+e^{-2x}} - 1 \quad (11)$$

Linear transfer function (Purelin):

$$Purelin(x) = x \quad (12)$$

Log-sigmoid transfer function (LogSig):

$$LogSig(x) = \frac{1}{1+e^{-x}} \quad (13)$$

3. PROPOSED METHODOLOGY

The proposed methodology can be resumed by the flowchart of Fig.6. It consists of: (1) decomposition of signals into three levels by WPD using Daubechies mother wavelet (db6). (2) Energies calculation and L-kurtosis of each terminal sub-band of WPD third level. (3) Classification of IM defects using MLP-NN, by giving energies and L-kurtosis values as inputs.

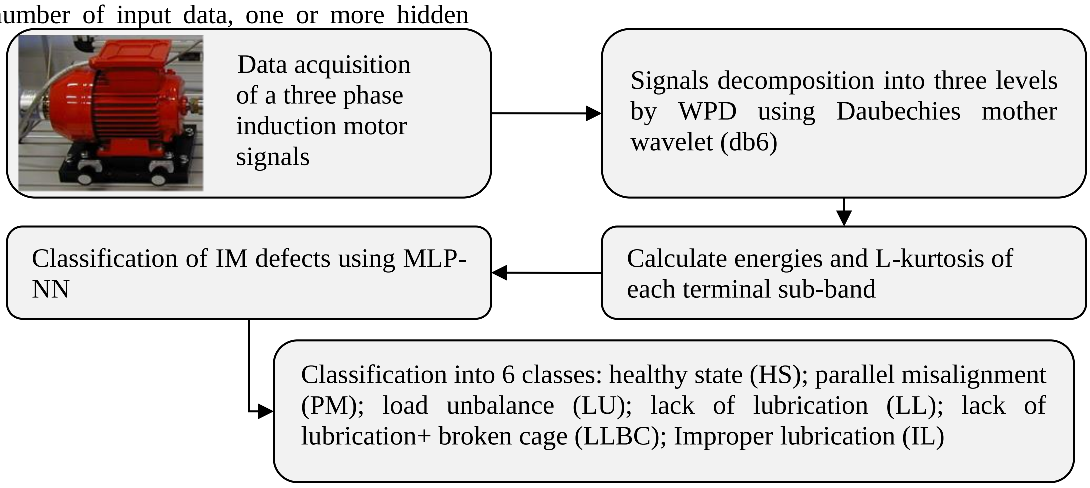

Fig. 6. Proposed methodology

4. EXPERIMENTAL SETUP FOR VIBRATORY SIGNALS ACQUISITION

The designed rig for vibratory signals acquisition shown in Fig.7 is composed from a typical cage induction machine (0.37 kW; 1 pole-pair; 380 V; 1.1A) with encoder, a PC, USB measuring device, accelerometer, elastic claw coupling, vibration analyzer, bearing unit, balanced flywheel (load) and Control unit which contains a frequency converter intended to regulate gradually the speed of rotation. The control unit also contains the rotation speed indicator and an another indicator for the power absorbed by the motor. The vibration signal used in this application, was measured at sampling frequency of 8 KHz, for two rotation speed 1500 rpm and 2000 rpm, under different operating conditions as represented in Table 4 and Fig. 8, where the defects were carried out as follow: the first bearing (A) was cleaned from its lubricant and its cage was broken manually, the second bearing (b) was just cleaned from lubricant, for the third one (c) fine grains of soil was added to the lubricant, to get a load unbalance (d) a weight of 2g has been added to the disc wheel and the parallel misalignment was executed using Adjuster for horizontal alignment of training shown in Fig. 8.e. The parameters of the bearing geometry are indicated in Table 2.

According to the parameters given in table 2 and the formulas (1) the characteristics bearing fault frequencies values are established in Table 3.

5. RESULTS AND DISCUSSIONS

In order to validate the proposed method, a set of vibration signals obtained from the rig shown in Fig.7 at different operating conditions (healthy state (HS); parallel misalignment (PM); load unbalance (LU); lack of lubrication (LL); lack of lubrication+ broken cage (LLBC); Improper lubrication (IL)) are exploited. For each case, 12 signals are measured, where each signal is composed from 820 samples. The 144 signals, in total, are decomposed by the WPD using the mother wavelet Daubchies 6 at depth of 3.

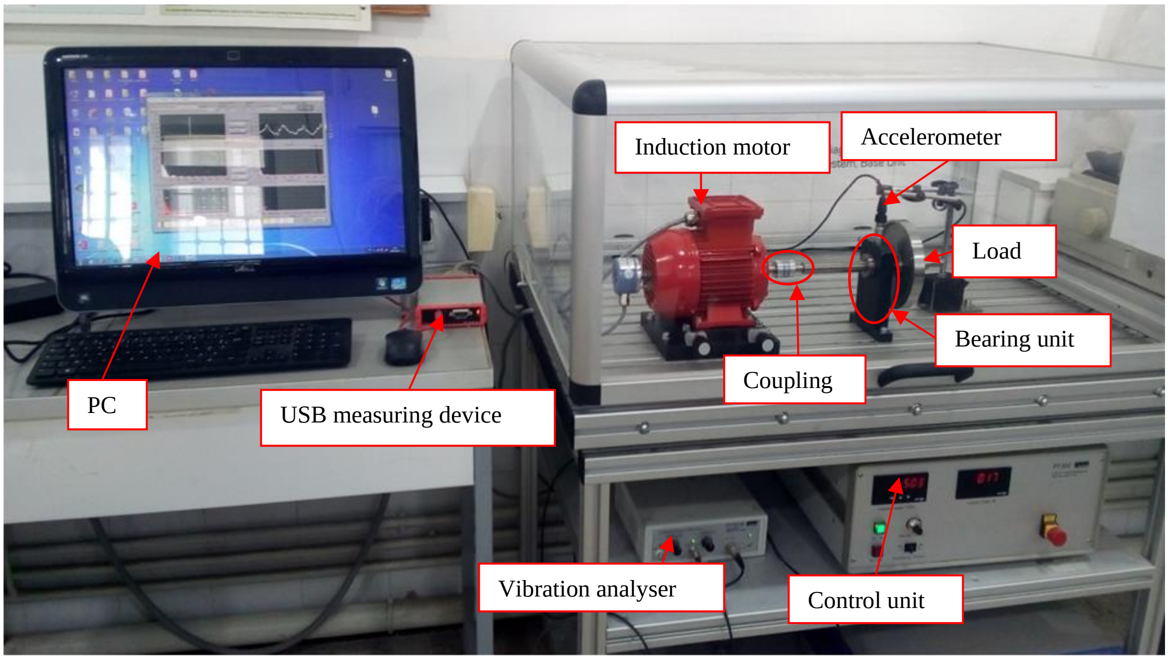

Fig. 7. Experimental setup

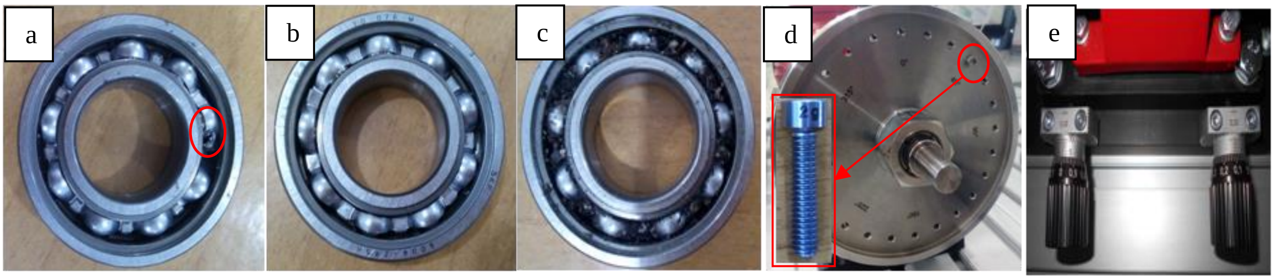

Fig. 8 IM defects: a) combined defects (lack of lubrication + broken cage), b) lack of lubrication, c) improper lubrication, d) load unbalance, e) parallel misalignment

Table 2. Bearin4g parameters: Ball bearing 6004-2RSH SKF

Inside diameter	Outside diameter	Thickness	Ball diameter	Pitch diameter
20	42	12	6	31

Table 3. Characteristics bearing fault frequencies

Rotation speed	**1500 rpm**	**2000 rpm**
Outer race fault frequency	90.73	120.96
Inner race fault frequency	134.27	179.01
Ball bearing fault frequency	62.16	82.88
Cage fault frequency	10.08	13.44

Table 4. Operating conditions of the collected data

		1500 rpm	2000 rpm
Healthy state		✓	✓
Parallel misalignment	0.5 mm	✓	✓
Load unbalance	2 g	✓	✓
Bearing defect	Luck of lubrication	✓	✓
	Luck of lubrication + broken cage	✓	✓
	Improper lubrication	✓	✓

Figures 9 and 10 present the original signal and the eight nodes resultant from the WPD at depth of three, of the two first cases: healthy state and parallel misalignment, at a rotational speed of 2000 rpm.

Through a visual comparison of the two figures 9 and 10, we remark that the amplitude of the original signal in the defective state as well as the signals resulting from the wavelet packet decomposition, are much more important than the vibratory signal amplitudes taken from the machine in a healthy state.

The different signals of the nodes are used to extract the values of energies and L-kurtosis in order to train the artificial neural network. Table 5 represents some values of the two indicators: energy and L-kurtosis, taken from the same sub-band for each operating condition, we have taken the example of the node (3, 0) where the values are most significant. It can be noticed that the increase in the severity of the defect treated, increases the value of the energy, the same for L-kurtosis, although the value of the energy increases intensively, the value of L-kurtosis varies slowly which prove its robustness to outliers.

These values variations helped the neural network presented in this paper to make the right classification decision.

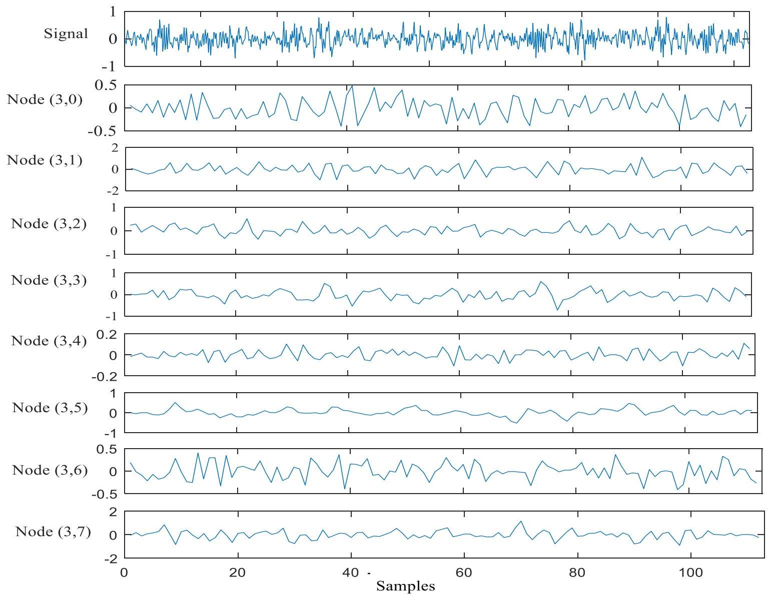

Fig. 9. Original signal and terminal sub-bands in a healthy state

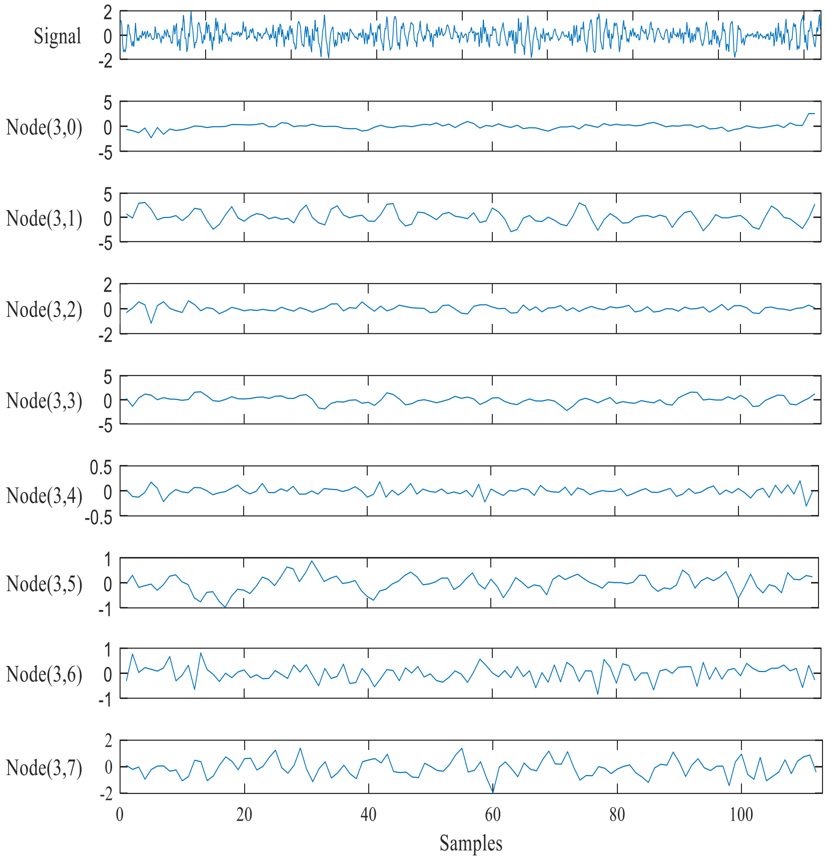

Fig. 10. Original signal and terminal sub-bands in case of parallel misalignment

Table 5. Samples of energy and L-kurtosis values

	HS	PM	LU	LL	LLBC	IL
Energy	5.526	22.542	498.996	59.328	269.487	619.726
L-kurtosis	0.091	0.100	0.137	0.108	0.134	0.144

The classifications of the IM defects are performed by Multi-Layer Perceptron neural network (MLP-NN) (Fig.11). Thus; 96 examples (signals) are used as training inputs and 48 examples as testing inputs, the rest of parameters used for neural networks are grouped in Table 6.

Table 6. MLP-NN design parameters

Learning type	Supervised
Activation function	
Hidden layer	Tansigmoid
Output layer	Purlin
Performance	MSE
Weights initialization	Random
Stopped criteria	
Minimum gradient	10^{-7}
Max.Epochs	1000
Mu	0.001

In order to facilitate the classification, the studied IM defects are coded as represented in Table 7.

The performance rate is defined by the ratio:

$$t_r\% = \frac{N_c}{N_t}100$$

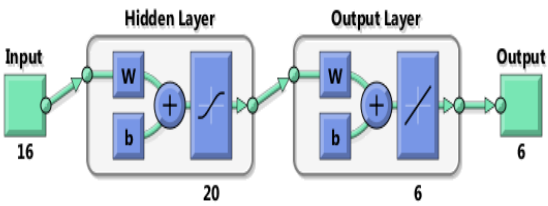

Fig. 11 MLP-NN architecture

Table 7. IM defects codification

IM conditions	class	Code classes
HS	1	100000
PM	2	010000
LU	3	001000
LL	4	000100
LLBC	5	000010
IL	6	000001

With: Nc: Number of correct classification and N_t: Number of total tests.

The experimental train and test outputs are shown in Fig.12, which illustrates how well the MLP-NN performs when classifying data according to the different sorts of faults(6 classes) is equal to 100 % with a total regression of 0.99893 (Fig.13) due to small errors that can be observed by the slight variation in values around the target outputs (Fig.14). The current findings attest to the efficiency of the suggested approach for classifying IM faults under various load circumstances.

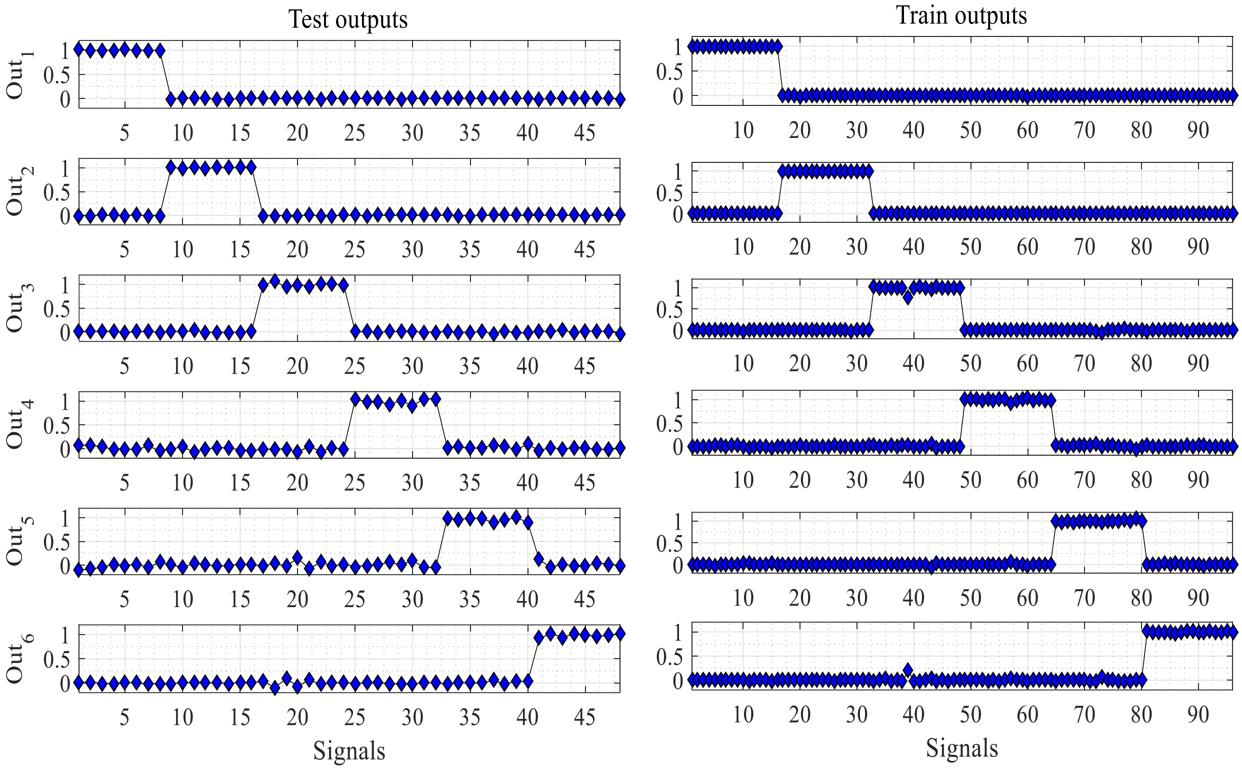

Fig. 12. Experimental train and test outputs

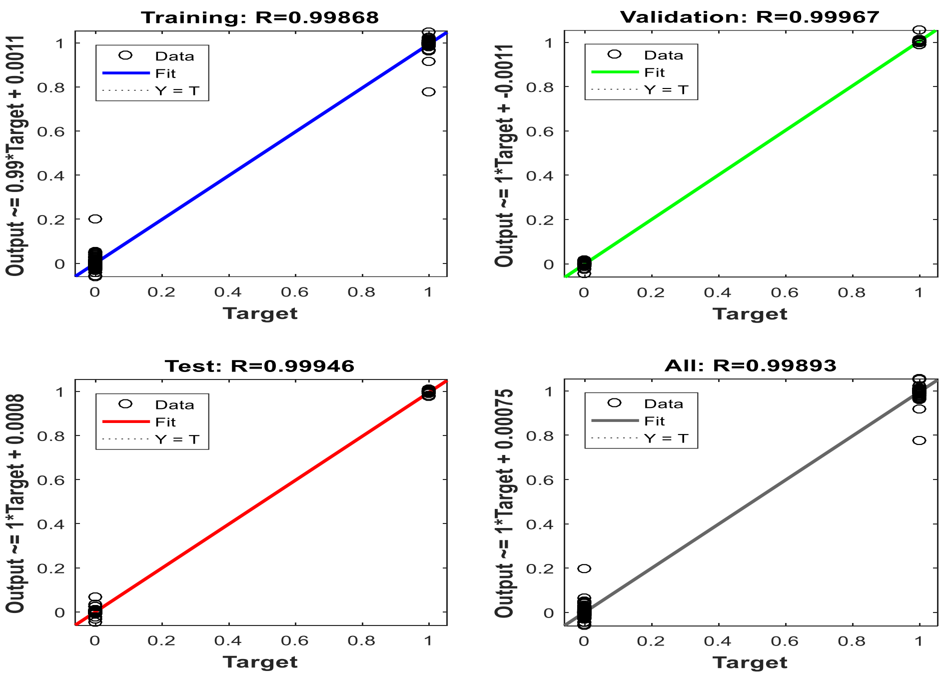

Fig. 13. Regression analysis

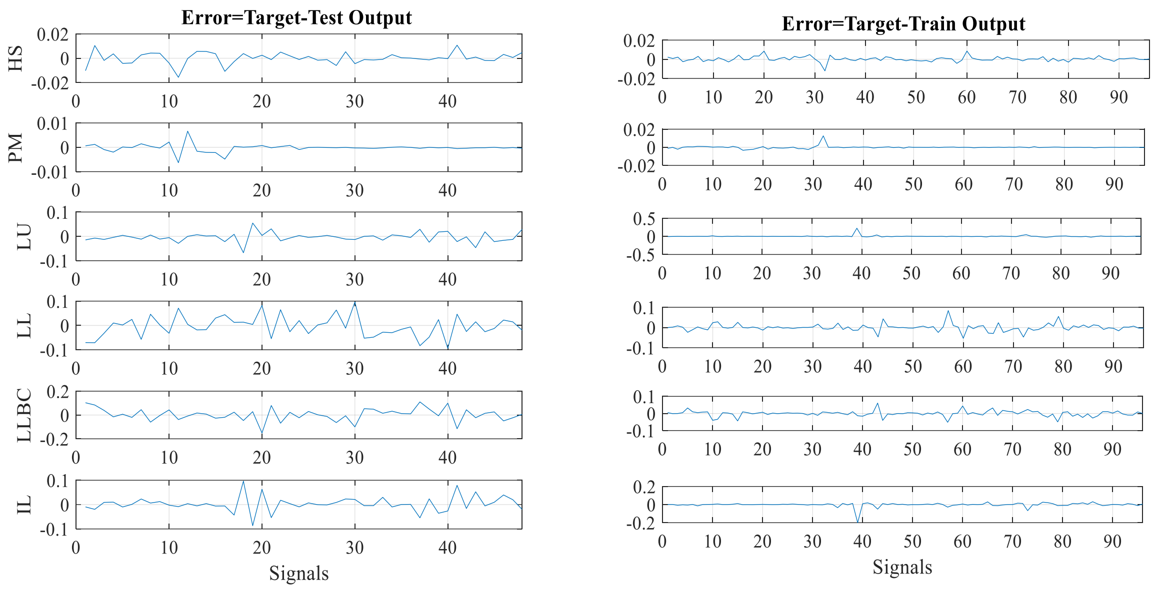

Fig. 14. Error between target and training and test output

6. CONCLUSION

This paper studied the efficiency of the proposed methodology, which is based on the combination of two methods of different types, the WPD and the multilayer perceptron neural networks, by introducing two statistical parameters: energy and L-kurtosis, calculated from each terminal sub-band of the WPD, as classifier inputs. This methodology was conducted on an induction motor running at two different speeds in order to detect three categories of defects: bearing defect, load unbalance and misalignment. The obtained results show the reliability of the proposed methodology, therefore, its application and use can be extended for the detection of other defects. The main challenge of this methodology is its capability to detect other combined defects using shorter signals (with the least number of samples).

Acknowledgement: *The authors would like to thank the Algerian General Direction of Research (DGRSDT) for providing the facilities and the financial funding of this project.*

Source of funding: *The Algerian General Direction of Scientific Research and Technological Development (DGRSDT).*

Author contributions: *research concept and design, B.M., M.L.; Collection and/or assembly of data, B.M., M.L.; Data analysis and interpretation, B.M.; Writing the article, B.N., S.S.; Critical revision of the article, S.S.; Final approval of the article, M.L., S.S.*

Declaration of competing interest: *The authors declare that they have no known competing financial interests or personal relationships that could have appeared to influence the work reported in this paper.*

REFERENCES

1. Siddiqui K, Sahay K, Giri V, Scholar P. Health monitoring and fault diagnosis in induction motor-a review. International Journal of Advanced Research in Electrical, Electronics and Instrumentation Engineering 2014; 3: 6549–65.
2. Zhang X, Wan S, He Y, Wang X, Dou L. Bearing fault diagnosis based on iterative 1.5-dimensional spectral Kurtosis. IEEE Access 2020; 8: 174233-174243. https://doi.org/10.1109/ACCESS.2020.3024697.
3. Feng H, Liang W, Zhang L. State monitoring and early fault diagnosis of rolling bearing based on wavelet energy entropy and LS-SVM. Journal of Computers 2013; https://doi.org/10.4304/jcp.8.8.2150-2155.
4. Kumar P, Hati AS. Dilated convolutional neural network based model for bearing faults and broken rotor bar detection in squirrel cage induction motors. Expert Systems with Applications 2022; 191: 116290. https://doi.org/10.1016/j.eswa.2021.116290.
5. He F, Ye Q. A bearing fault diagnosis method based on wavelet packet transform and convolutional neural network optimized by simulated annealing algorithm. Sensors 2022;22(4):1410. https://doi.org/10.3390/s22041410.
6. Zhang X, Li J, Wu W, Dong F, Wan S. Multi-fault classification and diagnosis of rolling bearing based on improved convolution neural network. entropy 2023; 25(5): 737. https://doi.org/10.3390/e25050737.
7. Belkacemi B, Salah S, Ghemari Z, Khazzane A. Detection of induction motor improper bearing lubrication by discrete wavelet transforms (DWT) decomposition. Instrumentation Mesure Metrologie 2020; 19: 347–54. https://doi.org/10.18280/i2m.190504.
8. Lin JL, Liu JYC, Li CW, Tsai LF, Chung HY. Motor shaft misalignment detection using multiscale entropy with wavelet denoising. Expert Systems with Applications 2010; 37(10): 7200–4. https://doi.org/10.1016/j.eswa.2010.04.009.
9. Zhao W, Hua C, Wang D, Dong D. Fault diagnosis of shaft misalignment and crack in rotor system based on MI-CNN. Proceedings of the 13th International

Conference on Damage Assessment of Structures. Lecture Notes in Mechanical Engineering. Springer Singapore 2020: 529-540. https://doi.org/10.1007/978-981-13-8331-1_39.
10. Lee Y, Kim BK, Bae JH, Kim K. Misalignment detection of a rotating machine shaft using a support vector machine learning algorithm. International Journal of Precision Engineering and Manufacturing 2021; 22. https://doi.org/10.1007/s12541-020-00462-1.
11. Lahouasnia N, Rachedi MR, Djalel D, Salah S. Load Unbalance Detection Improvement in Three-Phase Induction Machine Based on Current Space Vector Analysis. Journal of Electrical Engineering & Technology 2020; 15. https://doi.org/10.1007/s42835-020-00403-y.
12. Liu H, Mi X, Li Y. Comparison of two new intelligent wind speed forecasting approaches based on Wavelet Packet Decomposition, Complete Ensemble Empirical Mode Decomposition with Adaptive Noise and Artificial Neural Networks. Energy Conversion and Management 2018;155:188–200. https://doi.org/10.1016/j.enconman.2017.10.085.
13. Cherif H, Benakcha A, Laib I, Chehaidia SE, Menacer A, Soudan B, i in. Early detection and localization of stator inter-turn faults based on discrete wavelet energy ratio and neural networks in induction motor. Energy 2020; 212: 118684. https://doi.org/10.1016/j.energy.2020.118684.
14. Gao Q, Xiang J. A Method Using EEMD and L-Kurtosis to detect faults in roller bearings. 2018 Prognostics and System Health Management Conference (PHM-Chongqing). IEEE 2018 :71-76. https://doi.org/10.1109/PHM-Chongqing.2018.00018
15. Liu H, Xiang J. A strategy using variational mode decomposition, L-Kurtosis and minimum entropy deconvolution to detect mechanical faults. IEEE Access 2019; 7: 70564-70573. https://doi.org/10.1109/ACCESS.2019.2920064.
16. Bao W, Tu X, Hu Y, Li F. Envelope spectrum L-Kurtosis and its application for fault detection of rolling element bearings. IEEE Transactions on Instrumentation and Measurement 2020; 69(5): 1993–2002. https://doi.org/10.1109/TIM.2019.2917982.
17. Duan Z, Wu T, Guo S, Shao T, Malekian R, Li Z. Development and trend of condition monitoring and fault diagnosis of multi-sensors information fusion for rolling bearings: a review. The International Journal of Advanced Manufacturing Technology 2018; 96. https://doi.org/10.1007/s00170-017-1474-8.
18. Malla C, Panigrahi I. Review of condition monitoring of rolling element bearing using vibration analysis and other techniques. Journal of Vibration Engineering & Technologies 2019;7(4):407–14. https://doi.org/10.1007/s42417-019-00119-y.
19. Obaid R, Habetler TG. Effect of load on detecting mechanical faults in small induction motors. 2003 s. 307–11. https://doi.org/10.1109/DEMPED.2003.1234591.
20. Xu M, Marangoni RD. Vibration analysis of a motor-flexible coupling-rotor system subject to misalignment and unbalance, Part I: Theoretical Model And Analysis. Journal of Sound and Vibration 1994; 176(5): 663–79. https://doi.org/10.1006/jsvi.1994.1405.
21. Gangsar P, Tiwari R. Signal based condition monitoring techniques for fault detection and diagnosis of induction motors: A state-of-the-art review. Mechanical Systems and Signal Processing 2020; 144: 106908. https://doi.org/10.1016/j.ymssp.2020.106908.
22. Nandi S, Toliyat HA, Li X. Condition monitoring and fault diagnosis of electrical motors—A review. IEEE Transactions on Energy Conversion 2005; 20(4): 719–29. https://doi.org/10.1109/TEC.2005.847955.
23. Qin SR, Zhong YM. Research on the unified mathematical model for FT, STFT and WT and its applications. Mechanical Systems and Signal Processing 2004;18(6):1335–47. https://doi.org/10.1016/j.ymssp.2003.12.002.
24. Castejón C, Lara O, García-Prada JC. Automated diagnosis of rolling bearings using MRA and neural networks. Mechanical Systems and Signal Processing 2010; 24(1): 289–99. https://doi.org/10.1016/j.ymssp.2009.06.004.
25. Bae H, Kim YT, Lee SH, Kim S, Lee MH. Fault diagnostic of induction motors for equipment reliability and health maintenance based upon Fourier and wavelet analysis. Artificial Life and Robotics 2005; 9(3): 112–6. https://doi.org/10.1007/s10015-004-0331-7.
26. Bahoura M, Simard Y. Blue whale calls classification using short-time Fourier and wavelet packet transforms and artificial neural network. Digital Signal Processing 2010; 20(4): 1256–63. https://doi.org/10.1016/j.dsp.2009.10.024.
27. Gan M, Wang C, Zhu C. Construction of hierarchical diagnosis network based on deep learning and its application in the fault pattern recognition of rolling element bearings. Mechanical Systems and Signal Processing 2016; 72–73: 92–104. https://doi.org/10.1016/j.ymssp.2015.11.014.
28. Liu H, Shi Z. A fault detection approach using variational mode decomposition, L-kurtosis and random decrement technique for rotating machinery. International Journal of Mechanical Engineering and Applications 2020;8(1):16. https://doi.org/10.11648/j.ijmea.20200801.13.
29. Pang B, Tang G, Tian T. Rolling bearing fault diagnosis based on SVDP-Based Kurtogram and iterative autocorrelation of teager energy operator. IEEE Access 2019; 7: 77222-77237. https://doi.org/10.1109/ACCESS.2019.2921778.
30. Liu S, Hou S, He K, Yang W. L-Kurtosis and its application for fault detection of rolling element bearings. Measurement 2018; 116: 523–32. https://doi.org/10.1016/j.measurement.2017.11.049.
31. Orhan U, Hekim M, Ozer M. EEG signals classification using the K-means clustering and a multilayer perceptron neural network model. Expert Systems with Applications 2011; 38(10): 13475–81. https://doi.org/10.1016/j.eswa.2011.04.149.
32. Qiao W, Khishe M, Ravakhah S. Underwater targets classification using local wavelet acoustic pattern and Multi-Layer Perceptron neural network optimized by modified Whale Optimization Algorithm. Ocean 2021;219:108415. https://doi.org/10.1016/j.oceaneng.2020.108415.

Meriem BEHIM received her Master degree in Industrial Management and engineering in Maintenance and Reliability of Industrial technologies from École Superieure de Technologies Idustrielles (ESTI), Annaba, Algeria in 2019. She is currently pursuing the Ph.D. degree at the Laboratoire des Systems Eléctromécaniques (LSEM), Badji Mokhtar University, Annaba. Her Research interests include Electrical machines fault diagnosis And Signal processing.
e-mail: meriembehim96@gmail.com

Leila MERABET
received Engineer (electrical engineering) and Magister (electrical control) degrees from Annaba University in 1993 and 2001 respectively. She had her Ph.D degree in 2015 and the "Habilitation to supervise research" degree on electrical engineering in 2019. She is working as senior researcher "A". Her research interest includes renewable energy systems, power quality, harmonics, control, PV system, and artificial neuron networks.
She authored and co-authored many papers in academic journals, conferences and proceedings.
e-mail: lei_elt@yahoo.fr

Salah SAAD
received Ph.D. degree from Nottingham University UK in 1988. Since 1988 he worked as lecturer, senior lecturer then professor at Badji-Mokhtar Annaba University Algeria. He has conducted many researches projects in power electronics applications, electrical ac and dc drives as well as diagnosis and faults detection in ac machines and vibration sensors. His research interests are mainly in the area of power electronics such as harmonics elimination by active filters, PWM and Space vector modulation control, multilevel inverters and newconverter topologies. He has authored and coauthored many journal and conference papers.
e-mail: saadsalah2006@yahoo.fr